



## **Effect of mineral admixtures and aggregate natures on the behavior of high performance concrete**

**Y. Biskri<sup>1,\*</sup>, D. Achoura<sup>1</sup>, N. Chelghoum<sup>1</sup>, R. Jaubertie<sup>2</sup>**

<sup>1</sup>*Laboratoire de Matériaux, Géomatériaux et Environnement, Université de Badji Mokhtar Annaba, B.P. 12, Annaba 23000, Algeria.*

<sup>2</sup>*Laboratoire GCGM, INSA de Rennes, Rennes, France.*

*Received 23Sep 2015, Revised 06 May 2016, Accepted 10 May 2016*

*\*Corresponding author. E-mail: [biskriyasmina@yahoo.fr](mailto:biskriyasmina@yahoo.fr); Tel: (+213659472337)*

### **Abstract**

This paper presents the results of an experimental investigation carried out to evaluate the effectiveness of various types of coarse aggregates and mineral admixtures on properties of high performance concrete (HPC). For this purpose, three different coarse aggregate types (crystalline, pure and marl limestone) were used to produce HPC containing ground granulated blast-furnace slag (GGBFS) or silica fume mineral admixtures. The water to binder ratio is maintained at 0.27 for all mixtures. The different mixtures were tested for mechanical strength at different ages, while durability measurements such capillary absorption was also carried out. The experimental results showed that the production of HPC using limestone aggregate is therefore possible. The use of the Algerian blast furnace slag showed to be a good solution in terms of the material performance and it may offer a new approach to the valorization of this material in civil engineering construction. The GGBFS fillers contribute to improve the compactness of concretes and provide a relatively slow chemical activity. The microstructure analysis confirms all these findings.

*Key words:* High performance concrete, Blast furnace slag, silica fume, Mechanical behavior, aggregate's nature.

### **1. Introduction**

High performance concretes (HPC) are a new material largely used in the present time in civil engineering structures [1]. These concretes are obtained by the combination of mineral admixtures and Superplasticizer which increase the compressive strength more than 60 MPa and also improve workability and durability [2, 3]. Different types of mineral admixture are available (silica fume, fly ash, blast furnace slag. . .). The use of GGBFS in the manufacture of HPC is a new step forward in sustainable building construction. It offers the benefits of economical, technical and ecological considerations [4, 5]. GGBFS is interesting for its strength performance and its competitive price [6]. In literature review, GGBFS was used as chemical addition in HPC with a proportion of 10 to 20% weight of binder [1]. The proportion may vary depending on climate and environmental conditions. Also, silica fume (SF) is generally used together with a superplasticizer to control the workability [7, 8]. It enhances the early ages as well as the long-term properties of concrete. Taking in account cost and benefits; the optimum amount of silica fume is often 10% of binder mass [9].

In HPC formulations, aggregates by their high mass and volume fraction play a major role in the macroscopic behavior [10]. Strength, mineralogy, morphology and particle size distribution are the parameters involved in the choice of aggregates to obtain concrete with good characteristics [11]. The aggregate's nature influences the quality of the interfacial transition zone (ITZ). Limestone aggregates which are reactive have the strongest bonds with the cement paste due to the chemical reactions that occur over time and increase the adhesion forces [10, 12].

The aim was two folds: the first is economic concerned the recovery of granulated blast furnace slag from EL HADJAR by total replacement of silica fume in order to recommend an economical and sustainable solution to use the GGBFS in the formulation of HPC. The second is technique concerned a physico-mechanico and microstructural characterization in order to develop a HPC equivalent using local materials

## 2. Materials and experimental work

### 2.1. Binders

The binders include the Algerian Portland cements CEM II 42.5/A according to Algerian standard NA 442 [13] and two mineral admixtures. These were commercial silica fume (SF) according to NF EN 13263-1 [14] and the Algerian blast furnace slag (GGBFS). The glass content of Algerian slags is greater than 93% and therefore has a relatively slow hydraulic activity [6]. Table 1 describes the various properties of cement and mineral admixtures.

**Table 1:** Properties of cement and mineral admixtures.

| <b>Chemical composition (%)</b>                  |               |                    |                           |
|--|---------------|--------------------|---------------------------|
| <b>Component (%)</b>                             | <b>Cement</b> | <b>Silica fume</b> | <b>Blast furnace slag</b> |
| Silicon dioxide (SiO <sub>2</sub> )              | 21.91         | 99.01              | 34.41                     |
| Aluminum oxide (Al <sub>2</sub> O <sub>3</sub> ) | 5.19          | 0.03               | 8.17                      |
| Ferric oxide (Fe <sub>2</sub> O <sub>3</sub> )   | 2.94          | 0.05               | 4.15                      |
| Calcium oxide (CaO)                              | 60.41         | 0.02               | 40.69                     |
| Magnesium oxide (MgO)                            | 1.60          | 0.01               | 4.56                      |
| Sodium oxide (Na <sub>2</sub> O)                 | 0.16          | 0.04               | 0.10                      |
| Potassium oxide (K <sub>2</sub> O)               | -             | 0.15               | 0.89                      |
| Sulfur trioxide (SO <sub>3</sub> )               | 2.19          | 0.001              | 0.36                      |
| Cl <sup>-</sup>                                  | 0.02          | 0.009              | 0.01                      |
| Loss on ignition                                 | 3.83          | -                  | -                         |
| <b>Physical properties</b>                       |               |                    |                           |
| Fineness (cm <sup>2</sup> /g)                    | 3480          | 5000               | 3800                      |
| Bulk density (g/cm <sup>3</sup> )                | 1.020         | 0.5                | 1.22                      |
| Absolute density (g/cm <sup>3</sup> )            | 3.10          | 2.24               | 2.91                      |
| <b>Mechanical properties</b>                     |               |                    |                           |
| Pozzolanic activity index 7 day                  | -             | 1.05               | 0.88                      |
| Pozzolanic activity index 28 day                 | -             | 1.14               | 1.13                      |

### 2.2. Aggregates

Four different size fractions as 0/2 mm fine siliceous sand(SS), 1.25/5 mm crystalline limestone crushed sand (CLS), pure limestone crushed sand (PLS) and marl limestone crushed sand (MLS), 5/12, 5 mm and 12, 5/20 mm crystalline limestone gravel (CL), pure limestone gravel (PL) and marl limestone gravel (ML) of aggregates were used. Fig.1 shows the morphology of aggregates used and the fig .2 shows the particle size analysis of this aggregates.

The Chemical composition and physical properties of aggregates are shown in Tables 2 and 3. Physical properties were determined at University Civil Engineering laboratory and conducted according the European standard EN 12 620 [15]and the Los Angeles fragmentation coefficient LA determined according to standard NF-EN-1097-2 [16].



**Figure 1:** Morphology of aggregates used: A) Crystalline limestone, B) Pure limestone, and C) Marly limestone.

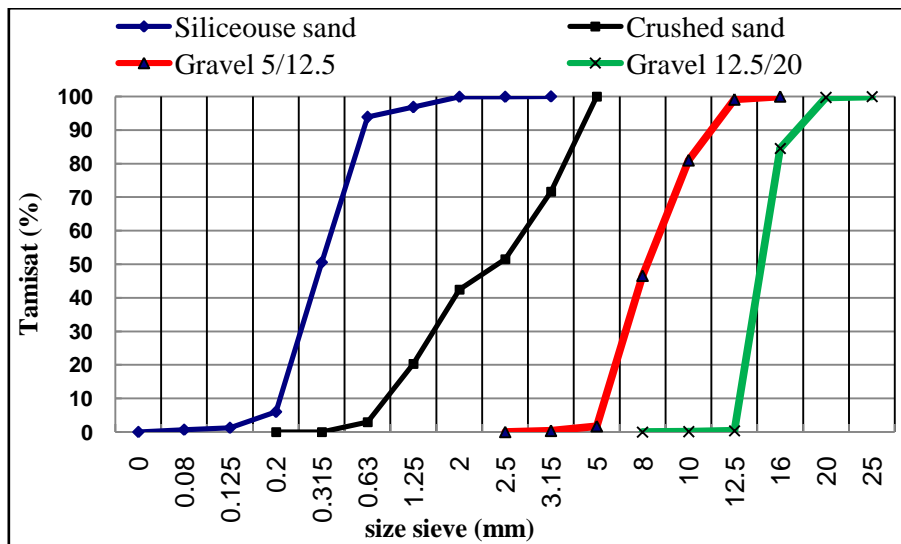


**Figure 2:** Particle size analysis of aggregates.

**Table 2:** Chemical composition of aggregates.

| Chemical composition (%)                         | PL    | CL   | ML   | SS    |
|--|-------|------|------|-------|
| Silicon dioxide (SiO <sub>2</sub> )              | 0.40  | 0.30 | 3.2  | 93.88 |
| Aluminum oxide (Al <sub>2</sub> O <sub>3</sub> ) | 0.11  | 0.44 | 1.3  | 2.13  |
| Ferric oxide (Fe <sub>2</sub> O <sub>3</sub> )   | 0.06  | 0.29 | 0.30 | 1.60  |
| Calcium oxide (CaO)                              | 55.91 | 53   | 49.6 | 0.43  |
| Magnesium oxide (MgO)                            | 0.18  | 1.6  | 1.4  | 0.12  |
| Sodium oxide (Na <sub>2</sub> O)                 | 0.05  | 0.1  | 0.2  | 0.24  |
| Potassium oxide (K <sub>2</sub> O)               | -     | 0.3  | 0.3  | 0.38  |
| Sulfur trioxide (SO <sub>3</sub> )               | 0.04  | -    | -    | 0.39  |
| TiO <sub>2</sub>                                 | -     | -    | -    | 0.13  |
| P <sub>2</sub> O <sub>5</sub>                    | -     | -    | -    | 0.03  |
| Loss on ignition                                 | 42.3  | 42.9 | 42.2 | 0.67  |

**Table 3:** Physical properties of aggregates.

| Property | Density (g/cm <sup>3</sup> ) | Fineness modulus (%) | Equivalent of sand (%) | Water Absorption (%) | Los-Angeles test (%) | Flattening Coefficient (%) |
|----------|------------------------------|----------------------|------------------------|----------------------|----------------------|----------------------------|
| SS       | 2.56                         | 1.95                 | 90                     | -                    | -                    | -                          |
| CLS      | 2.7                          | 4.33                 | 97                     | -                    | -                    | -                          |
| PLS      | 2.94                         | 4.25                 | 97                     | -                    | -                    | -                          |
| MLS      | 2.6                          | 4.32                 | 96                     | -                    | -                    | -                          |
| CL       | 2.65                         | -                    | -                      | 0.46                 | 26                   | 3.23                       |
| PL       | 2.69                         | -                    | -                      | 0.20                 | 24                   | 3.01                       |
| ML       | 2.60                         | -                    | -                      | 0.76                 | 27                   | 4.2                        |

### 2.3. Concrete mixtures

The HPC mix design was determined using an adjusted SHERBROOK method [17]. A constant water–binder ratio (W/B) of 0.27 was investigated for HPC samples prepared with silica fume or GGBFS mineral admixtures. Dosage of 10% silica fume and 20% GGBFS were used in the preparation of different HPC samples. A cement and mineral admixture binder content of 520 kg/m<sup>3</sup> was fixed. The super-plasticizer VISCOCRETE TEMPO 12 according to the European standard NF EN 934-2 [18] was used in all HPC. Table 4 gives the mix proportions of the concretes developed in this study.

**Table 4:** Mix proportion of concrete mixtures.

| Material           | Unit | HPCCLSF | HPCPLSF | HPCMLSF | HPCCLBS | HPCPLBS | HPCMLBS |
|--------------------|------|---------|---------|---------|---------|---------|---------|
| Cement             | Kg   | 470     | 470     | 470     | 416     | 416     | 416     |
| Fine sand          | Kg   | 360     | 380     | 346     | 370     | 390     | 350     |
| Crushed sand       | Kg   | 370     | 390     | 345     | 371     | 390     | 351     |
| Gravel1 (5/12.5)   | Kg   | 430     | 416     | 344     | 430     | 416     | 344     |
| Gravel (12.5/20)   | Kg   | 620     | 634     | 706     | 620     | 634     | 706     |
| Blast furnace slag | %    | -       | -       | -       | 20      | 20      | 20      |
|                    | Kg   | -       | -       | -       | 104     | 104     | 104     |
| Silica fume        | %    | 10      | 10      | 10      | -       | -       | -       |
|                    | Kg   | 50      | 50      | 50      | -       | -       | -       |
| Superplasticizer   | %    | 1.2     | 1.2     | 1.2     | 1.2     | 1.2     | 1.2     |
|                    | Kg   | 6.25    | 6.25    | 6.25    | 6.25    | 6.25    | 6.25    |
| Water              | L    | 145     | 145     | 145     | 145     | 145     | 145     |
| W/B                | /    | 0.27    | 0.27    | 0.27    | 0.27    | 0.27    | 0.27    |

HPCCLSF: High Performance Concrete with crystalline limestone and aggregates Silica fume.

HPCPLSF: High Performance Concrete with pure limestone aggregates and Silica fume.

HPCMLSF: High Performance Concrete with marly limestone aggregates and Silica fume.

HPCCLBS: High Performance Concrete with crystalline limestone aggregates and Blast furnace slag.

HPCPLBS: High Performance Concrete with pure limestone aggregates and Blast furnace slag.

HPCMLBS: High Performance Concrete with marly limestone aggregates and Blast furnace slag.

### 2.4. X-ray diffraction analysis (XRD)

X-ray diffraction test is carried out on mineral admixtures and aggregate's powder. The Philips PW 3710 diffract meter is provided with a Cu anticathode and a Ni filter. Its wave length is  $\lambda = 1.54 \text{ \AA}$ . The Recording is performed Step by step between 5° and 70 ° 2 $\theta$  for a period of time of one hour and half. The characterization of mineral admixtures by the XRD analysis show that the Algerian blast furnace slag has a low amount of phases crystallized presented in the form of calcite and metallic iron (Fig.3) , and the commercial silica fume has a low amounts of minerals crystallized presented in the form of tridymite and cristobalite (Fig.4).

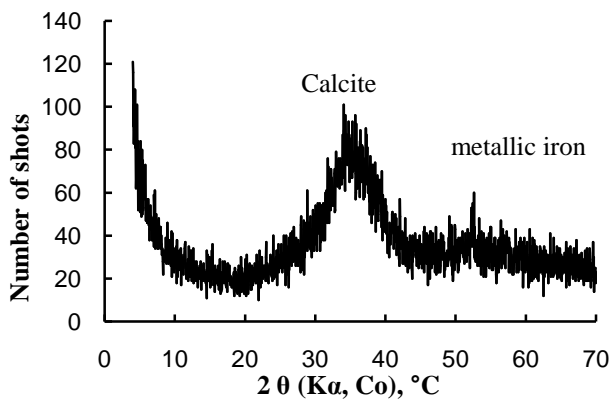


**Figure 3:** XRD Diagram of blast furnace slag [19].

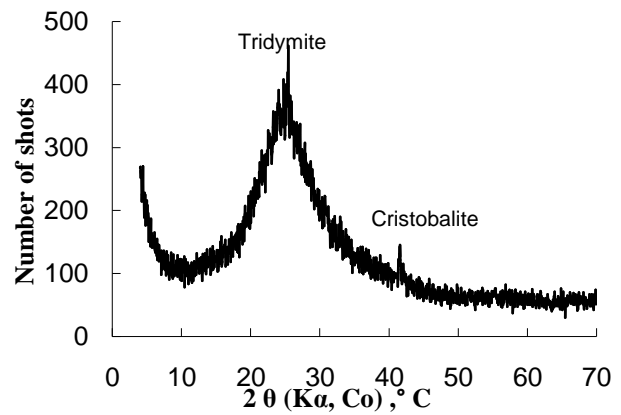


**Figure 4:** XRD Diagram of silica fumes [19].

The characterization of aggregate's mineralogy show that pure limestone is almost consisting of calcium carbonate (Fig.5) unlike gray crystalline limestone which presents some dolomite (Fig.6) and black marly limestone which shows both the presence of dolomite and quartz (Fig.7).

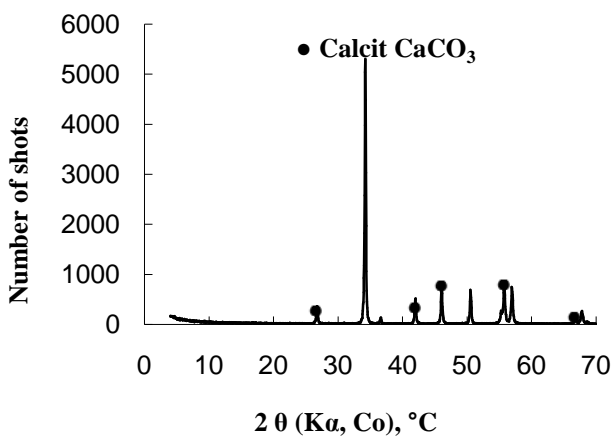


**Figure 5:** XRD Diagram of pure limestone.

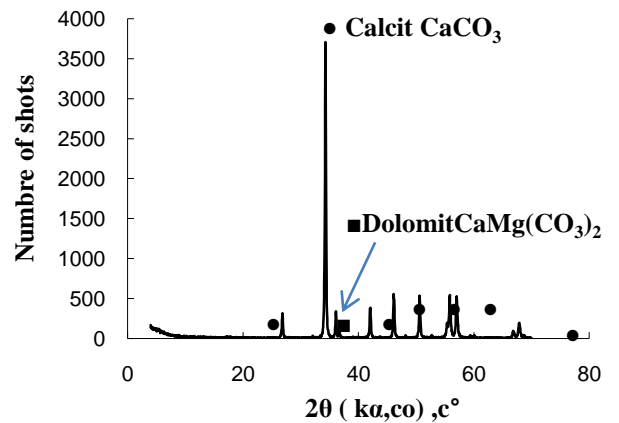


**Figure 6:** XRD Diagram of crystalline limestone.

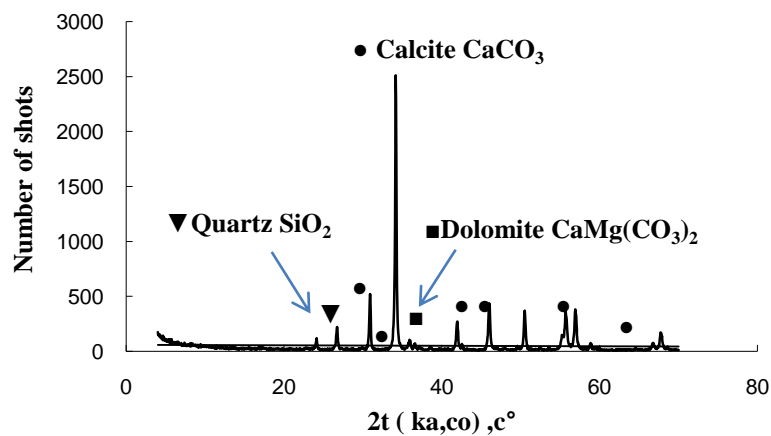


**Figure 7:** XRD Diagram of marly limestone

**2.5. Specimens and test program**

For each mixture, cube specimens 100 x 100 x 100 mm<sup>3</sup> were used to determine the compressive strength, according to EN 12390-3 [20], 150 x 150 x 500 mm<sup>3</sup> specimens were used to determine the flexural strength, according to EN12390-5 [21], a STRASSENTEST electromechanical testing machine with capacity of 50 kN was used (Fig.8) .All the specimens were cast in steel molds and compacted on a vibration table. They were demoulded after about 24 h and moist cured at 20°C and 100% RH for 28 days. For all hardened testing results, the average value of experimental results from three identical specimens was adopted. Durability performance was evaluated by measuring the capillary absorption; Concrete discs of 15 x 5 cm were used to determine the capillary absorption.



**Figure 8:** Machine of flexural strength.

**3. Results and discussion**

**3.1. Fresh concrete**

The slump of the fresh concrete for the different concrete mixtures is shown in Table 5.

**Table 5:** Properties of fresh concrete mixtures.

| Concrete | Slump test (mm) | Fresh concrete density (kg/m <sup>3</sup> ) | Air content (%) |
|----------|-----------------|---|-----------------|
| HPCCLSF  | 250             | 2490  | 2               |
| HPCPLSF  | 230             | 2500  | 1.8             |
| HPCMLSF  | 200             | 2470  | 2.2             |
| HPCCLBS  | 200             | 2525  | 1.7             |
| HPCPLBS  | 180             | 2530  | 1.6             |
| HPCMLBS  | 160             | 2510  | 2               |

It could be observed that the HPC has a slump test of around 220 to 250 mm. HPC with GGBFS showed a less slump loss than the one with silica fume which was probably due to the rough texture and micro-porosity of GGBFS particles as shows in (Fig.9) .

GGBFS or silica fume mineral admixtures improve significantly the compactness of HPC. The density of HPC depends on the nature of the components used in the formulation, it can be see that the density of HPC with GGBFS mineral admixture is higher than the HPC samples with silica fume, for the same type of aggregate the density depends on the nature of the additions used and therefore the difference is mainly due to the intrinsic density of the GGBFS which is superior to that of silica fume.

Table 5 also shows the effect of crystalline, pure and marl limestone on the air content of fresh concrete. The mineralogy of aggregates did not affect the air content of HPC.

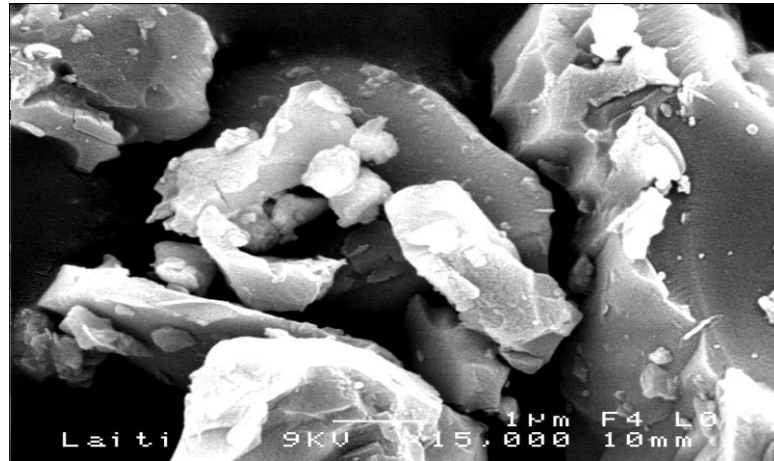


**Figure9:** SEM image of GGBFS particles.

### 3.2. Capillary absorption

The absorption coefficient versus the square root of time is presented in Fig. 10.

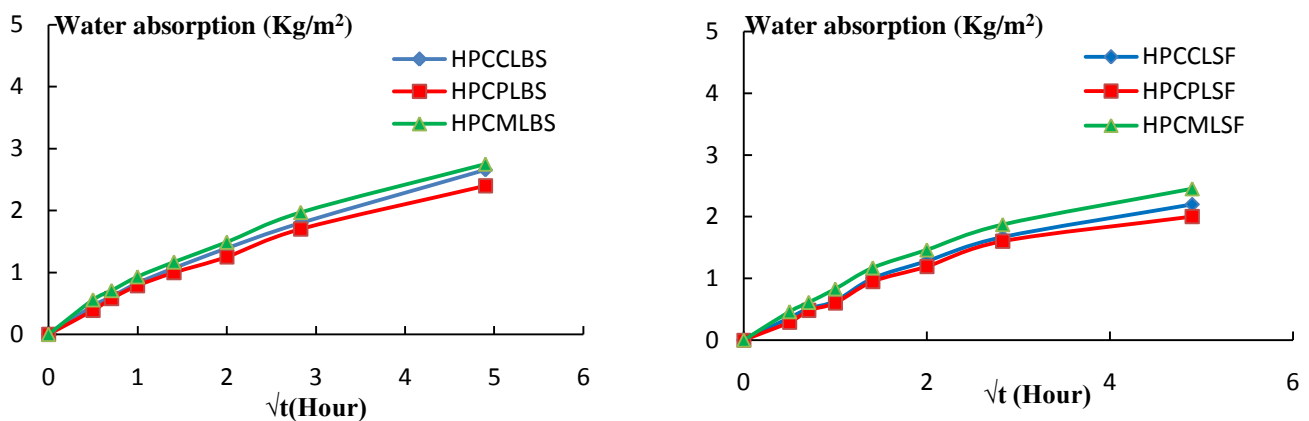


**Figure 10:** Capillary absorption of HPCBS and HPCSF.

Fig. 10 shows a succession of linear segments characterized by a decrease in slopes. This decrease can be explained by a slower absorption phenomenon. HPC have very low porosity. Most of the voids are disconnected resulting in low absorption of water by capillarity for both types of fillers.

The Capillary absorption is primarily concerned with the capillary voids. The short duration of the test, which is 24 hours, does not allow the small diameter gel voids filling. The hydraulic or pozzolanic activities of mineral admixtures promote slower HPC absorption velocity. In fact, the capillary voids surface is covered by CSH produced during chemical reactions of mineral admixtures. The use of GGBFS and silica fume mineral admixtures significantly reduces the absorption velocity by improving the porous structure; these results are consistent with the literature [9, 19, 22].

Fig. 10 also shows that the sample with the minimum rate of absorption was the HPC with pure limestone aggregate probably because the good adhesion between cement past and pure limestone in blocking the continuity of the capillary in size pores.

### 3.3. Compressive strength

The results of the compressive tests are given in Table 6. The coefficient of variation varies in the range between the 0.16% and the 1.46%, which means that there was no size effect.

**Table 6:** Cube compressive peak strength.

| Specimens | Strength at 28 days (MPa) | Mean value (MPa) | Standard deviation (MPa) | Coefficient of variation (%) |
|-----------|---------------------------|------------------|--------------------------|------------------------------|
| HPCCLSF-1 | 63.69                     | 62.80            | 0.92                     | 1.46                         |
| HPCCLSF-2 | 61.86                     |                  |                          |                              |
| HPCCLSF-3 | 62.86                     |                  |                          |                              |
| HPCPLSF-1 | 67.76                     | 67.52            | 0.54                     | 0.80                         |
| HPCPLSF-2 | 66.9                      |                  |                          |                              |
| HPCPLSF-3 | 67.9                      |                  |                          |                              |
| HPCMLSF-1 | 62                        | 61.54            | 0.54                     | 0.87                         |
| HPCMLSF-2 | 60.95                     |                  |                          |                              |
| HPCMLSF-3 | 61.67                     |                  |                          |                              |
| HPCCLBS-1 | 60.95                     | 60.8             | 0.30                     | 0.50                         |
| HPCCLBS-2 | 60.45                     |                  |                          |                              |
| HPCCLBS-3 | 61                        |                  |                          |                              |
| HPCPLBS-1 | 62.2                      | 62.1             | 0.10                     | 0.16                         |
| HPCPLBS-2 | 62.1                      |                  |                          |                              |
| HPCPLBS-3 | 62                        |                  |                          |                              |
| HPCMLBS-1 | 60                        | 60.15            | 0.26                     | 0.43                         |
| HPCMLBS-2 | 60.45                     |                  |                          |                              |
| HPCMLBS-3 | 60                        |                  |                          |                              |

Fig. 11 shows the average compressive strength for the different mixes using crystalline, pure and marl limestone as coarse aggregate and both silica fume or GGBFS mineral admixtures.

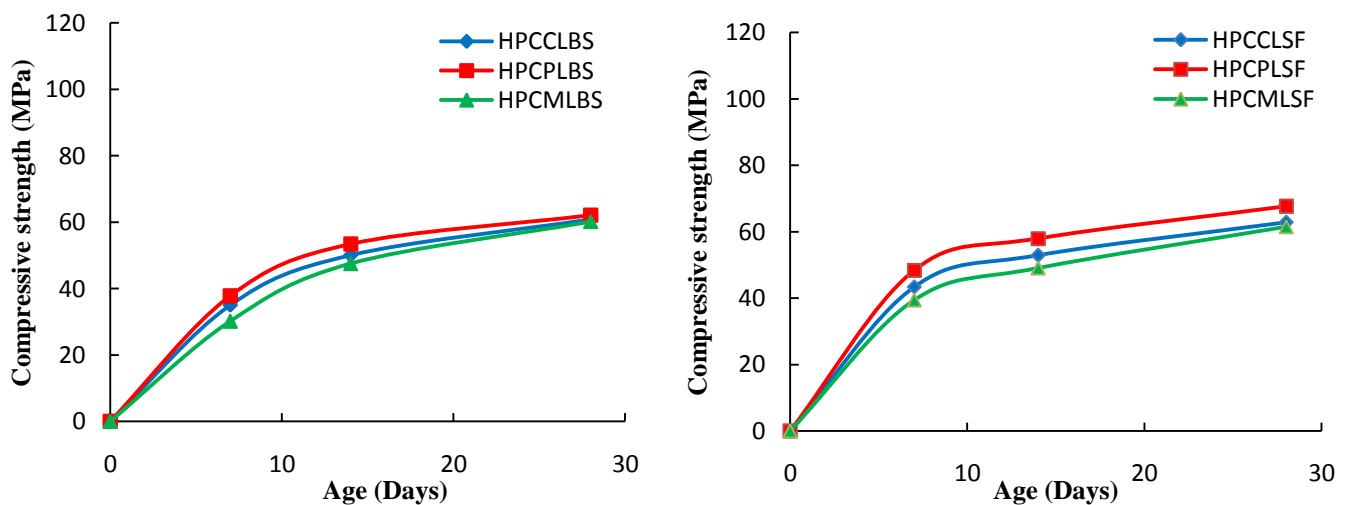


**Figure 11:** Variation of compressive strength of HPCBS and HPCSF.

It can be seen that the compressive strength for all HPC mixes increases with the curing time due to the cement hydration and accumulation of hydration products closing up some of available pore spaces in concrete matrix resulting in improving the mechanical performance.

The rate of strength development in HPC depends on the pozzolanic and hydraulic activity of mineral admixtures as well as the physical and mechanical properties of the aggregates.

The compressive strength varied from 62.80MPa, 67.52MPa and 61.54MPa for HPC with crystalline limestone, pure limestone and marly limestone aggregate respectively and silica fume, to 60.80MPa, 62.10MPa and 60.15MPa for HPC with the same aggregate and GGBFS. The increase in the compressive strength could be attributed firstly, to the pozzolanic and hydraulic effect of mineral admixtures; the compressive strength of HPC with silica fume is higher than that with GGBFS, due to the high fineness and high silica content of silica fume compared to GGBFS, at normal temperature, the pozzolanic reaction of GGBFS is a slow process also the difference in the hydration process of the two mineral admixtures. The hydration in the presence of silica fume can be divided into two phases: the first one is characterized by a rapid hydration and dissolution accompanied by a consumption of silica fume particles and an increase of mechanical strength. The second phase is characterized by a small change of hydration but in the same time the system becomes denser as a result of the hydration products rearrangement and the change of large pores into fine pores due to the pozzolanic reaction, which has an important role in the strength increase.

In contrast, the vitrified blast furnace slag is rapidly soluble in alkaline water and therefore needs the addition of an activating agent to develop satisfactory kinetic hydration (in this case is the cement).

The hydration is relatively a slow process occurring as repetition of dissolution-concentration-precipitation cycles during years until a maximum hydration of slag grains is reached.

GGBFS particles are smoother than the ones of clinker, hydrates found some difficulties to develop on these particles and consequently, the development of mechanical strength of cement-slag HPC is slow compared to cement-silica fume HPC. These confirmed the results obtained by [23].

Secondly, to the strong adhesion between the textures of pure limestone and cement paste that lead to improve the transition zone in concrete. Pure limestone has a higher density and low porosity, and also these aggregates with very rough compact morphology as illustrated by the SEM-image in fig11B. As a result, the aggregate's liaison in the matrix is improved which can enhance the mechanical behavior. For HPC, the mechanical strength of the cementitious matrix is greater than that of aggregates, thus the mechanical strength of HPC depends of the resistance of the aggregates.

The study of MEKANI, Gaweska and Manso [10, 24, 25] confirmed that the mineralogy of pure limestone aggregate is constituted mainly of carbonates which results in excellent mechanical behavior of aggregates with low porosity. In addition, the calcite of CSH germination in epitaxial occurs more easily in contact with calcite crystals of limestone aggregate. This phenomenon would result in a strong bond between the calcite and the CSH at the interface and therefore a very resistant ITZ.

### 3.4. *Flexural behavior*

Three point bending tests were performed on the prismatic specimens. The mean values for HPC with silica fume are slightly higher than the HPC with GGBFS (Table 7).

It can be seen that the best strengths are obtained with HPC prepared with pure limestone aggregates and silica fume. The type of mineral admixtures have a very slightly influence on the flexural behavior, also the quality of the aggregate-cement matrix adhesion, which depends on the mineralogical, mechanical and morphological properties of aggregates.

The behavior of the HPC specimens with GGBFS and SF mineral admixture was almost linear-elastic up to the peak load, followed by a sudden decrease in strength and a complete separation of specimens into two parts.

**Table 7:** Three point bending tests: peak loads.

| Specimens | Peak loads (kN) | Mean value (kN) | Standard deviation (kN) | Coefficient of variation (%) | Modulus of rupture (MPa) |
|-----------|-----------------|-----------------|-------------------------|------------------------------|--------------------------|
| HPCCLSF-1 | 21              | 19.5            | 1.29                    | 6.58                         | 4.34                     |
| HPCCLSF-2 | 19              |                 |                         |                              |                          |
| HPCCLSF-3 | 18.6            |                 |                         |                              |                          |
| HPCPLSF-1 | 25.2            | 24.0            | 1.11                    | 4.60                         | 5.34                     |
| HPCPLSF-2 | 23              |                 |                         |                              |                          |
| HPCPLSF-3 | 23.9            |                 |                         |                              |                          |
| HPCMLSF-1 | 19              | 18.0            | 1.00                    | 5.56                         | 4.00                     |
| HPCMLSF-2 | 17              |                 |                         |                              |                          |
| HPCMLSF-3 | 18              |                 |                         |                              |                          |
| HPCCLBS-1 | 21              | 19.0            | 1.70                    | 8.95                         | 4.23                     |
| HPCCLBS-2 | 18.1            |                 |                         |                              |                          |
| HPCCLBS-3 | 18              |                 |                         |                              |                          |
| HPCPLBS-1 | 23.8            | 21.5            | 2.02                    | 9.41                         | 4.78                     |
| HPCPLBS-2 | 20.7            |                 |                         |                              |                          |
| HPCPLBS-3 | 20              |                 |                         |                              |                          |
| HPCMLBS-1 | 18.7            | 17.5            | 1.01                    | 5.77                         | 3.90                     |
| HPCMLBS-2 | 16.9            |                 |                         |                              |                          |
| HPCMLBS-3 | 17              |                 |                         |                              |                          |

Fig. 12 shows the average load–deflection curves for both SF and GGBFS mineral admixtures.

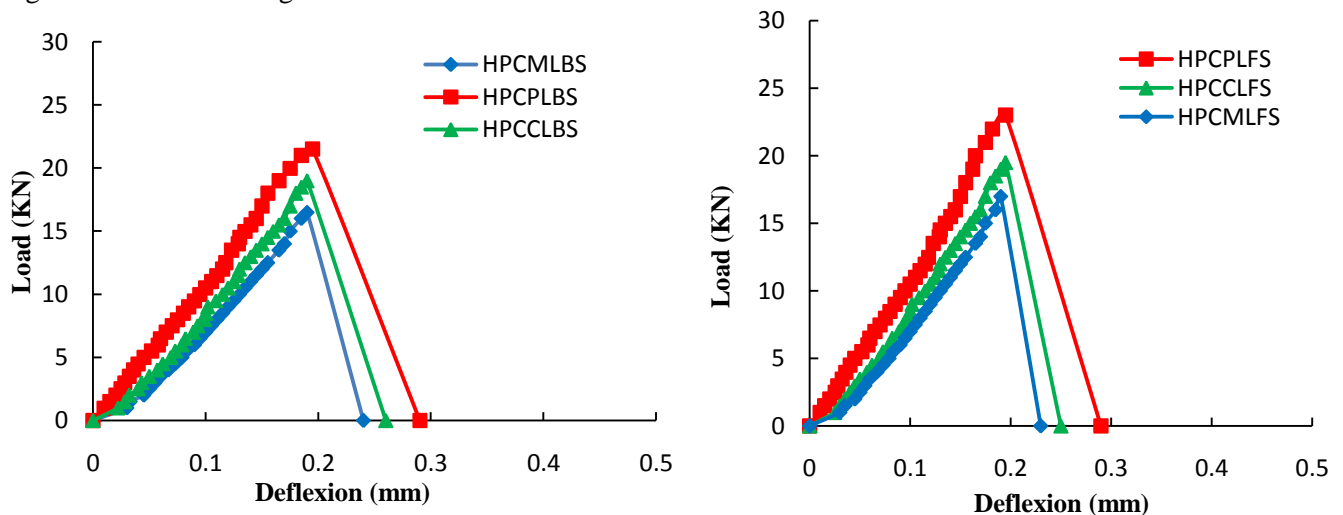


**Figure 12:** Load–deflection curves of HPCBS and HPCSF.

#### 4. Microstructure by SEM

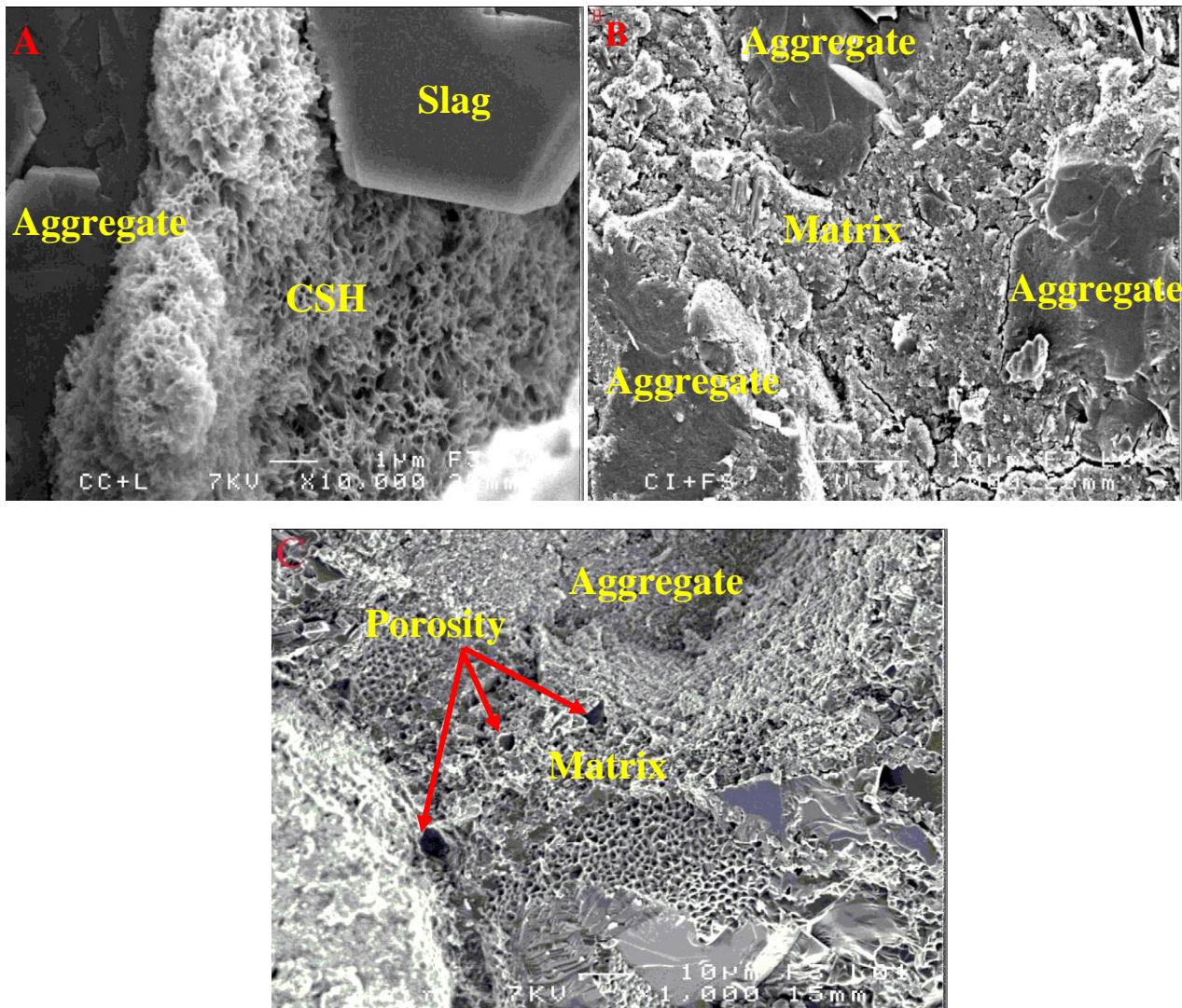
The microstructure analysis of HPC prepared with crystalline, pure and Marly limestone aggregates cured in tap water for 28 days are shown in Fig. 13(A), (B), (C) respectively.

Fig 13A shows a good bond between the matrix and crystalline limestone aggregate with the presence of some anhydrate slag particles, the CSH are well structured as foam. Fig.13B shows the microstructure of HPC with pure limestone and silica fume. the interfacial transition zone (ITZ) between the particles of coarse aggregate

and the cement matrix, the compactness of the cementitious matrix which presents a minimum of voids and aggregates matrix bonding can be seen.

Fig.13C shows the microstructure of HPC with Marly limestone and silica fume, it can be seen the interfacial transition zone (ITZ) between the particles of coarse aggregate and the cement matrix, and the presence of some porosity.

The microstructure of HPC shows a dense and compact microstructure, this later can be attributed to: the filler effect and pozzolanic activity, a filling of ITZ and the microcracks formed on the HPC surface, the optimized size distribution and finally a low E/B ratio.



**Figure 12:**SEM images of HPC with A) crystalline limestone, B) pure limestone and C) Marly limestone.

## Conclusions

The study presented in this paper is a contribution to a better understanding on the effects of aggregate's nature and mineral admixtures on the HPC behavior. Marl, crystalline and pure limestone aggregates and silica fume or GGBFS were investigated. The following conclusions are drawn based on the results of different tests and analysis:

1. The physical properties of pure limestone aggregate(water absorption, loss- angels test) were superior to those of crystalline and marl limestone aggregates. However, the bulk specific gravity of the pure limestone aggregate was more than that of the latter aggregates.

2. The unit weight of HPC with pure limestone aggregate was more than that of crystalline and marl limestone aggregate. The increase in unit weight due to apparent specific density of pure limestone ( $2690 \text{ kg/m}^3$ ), reaching unit weight up to  $2530 \text{ kg/m}^3$ .
3. HPC with pure limestone aggregate show the best compaction characteristics and strength properties. This is the results of the intrinsic aggregate's properties. The pure limestone shows stronger bonds with the cement paste. These later increase the adhesion forces of and consequently improve the quality of the interfacial transition zone.
4. HPC with GGBFS mineral admixture have good mechanical properties similar than the one obtained with the silica fume therefore can be recommended to use GGBFS as mineral admixture in the formulation of HPC and it can be substituted the silica fume by blast furnace slag.

**Acknowledgements** - The authors express their thanks to Jonny Loic and Francis Goutefangeas, CMEBA Rennes1 University (France) and LMDC, Toulouse, for their assistance with SEM and XRD.

## References

1. Aïtcin P.C., *London, New York: E. & F.N. Spon.* (1998) 591.
2. Chen B., Liu J., *Constr.Build.Mater.* 22 (2008) 1108–13.
3. Vejmelkova E., Pavlikova M., Keršner Z., Rovnanikova P., Ondracěk M., Sedlmajer M., et al., *Constr. Build.Mater.* 23 (2009) 2237–45.
4. Chidiac S.E., Panesar D.K., *Cem .Concr. Compos.* 30 (2008) 63–71.
5. Bernal S., De Gutierrez R., Delvasto S., Rodriguez E., *Constr. Build.Mater.* 24 (2010) 208–14.
6. Achoura D.J., *Matériaux. et. Techniques.* 96(2009) 189–199.
7. Hassan K.E ., Cabrera J.G., Maliehe R.S., *Cem. Concr. Compos.* 22 (2000) 267–71.
8. Kořksal F., Altun F., Yiğitü I., Şahin Y., *Constr. Build .Mater.* 22 (2008) 1874–80.
9. Kaikea A., Achoura D.j., Duplan F., Rizzuti L., *Materials .and. Design.* 63 (2014) 493–499.
10. Makani A., Vidal T., Pons G., Escadeillas G., *International Conference on Experimental Mechanics, Poitiers.* 2010.
11. Alexander M.G., *Journal of A.C.I. Materials,* 9 (1996) 569-577.
12. Abdulrahman M., Alhozaimy., *Cement. &.Concrete. Composites .*31 (2009) 470–473.
13. NA 442. 2005. Ciment. (2005).
14. NF EN 13263-1. Fumée de silice pour béton. (2009).
15. EN 12 620. European Standards, Aggregates for Concrete. (2002).
16. Aïctin. P.C., *Editions Eyrolles.* (2001)683p.
17. NF EN 1097-2. Tests for Mechanical and Physical Properties of Aggregates. (2010).
18. NF EN 934-2. High range Water Reducing/Superplasticized Concrete Admixture. (2012).
19. Ali Boucetta T., Thèse de doctorat, Université d'Annaba, Algérie. (2014).
20. BS EN 12390-3. Testing hardened concrete. Compressive strength of test specimens. (2009).
21. BS EN 12390-5. Testing hardened concrete. Flexural strength of test specimens. (2009).
22. Matos A.M., sousa-coutinho J., *Construction.And. Building Materials.* 36 (2012) 205-215.
23. Abo-El-Enein S.A., Gamal El-kady T.M., El-Sokkary, Mahmoud Gharie, *H.B.R.C. Journal.* 11 (2015) 7–15.
24. Gaweska H., Thèse de doctorat, ENPC, Paris. (2004).
25. Maso J., London. *New York: Spon.* (1996).

(2016) ; <http://www.jmaterenvirosci.com/>